

AD-A283 626



1

ARMY RESEARCH LABORATORY



A Uniaxial Nonlinear *Thermoviscoelastic* Constitutive Model With Damage for M30 Gun Propellant

George A. Gazonas

ARL-TR-469

June 1994

DTIC
ELECTE
AUG 24 1994
S B D

3919/94-26922



DTIC QUALITY INSPECTED 8

APPROVED FOR PUBLIC RELEASE; DISTRIBUTION IS UNLIMITED.

94 8 23 1 1 4

NOTICES

Destroy this report when it is no longer needed. DO NOT return it to the originator.

Additional copies of this report may be obtained from the National Technical Information Service, U.S. Department of Commerce, 5285 Port Royal Road, Springfield, VA 22161.

The findings of this report are not to be construed as an official Department of the Army position, unless so designated by other authorized documents.

The use of trade names or manufacturers' names in this report does not constitute indorsement of any commercial product.

REPORT DOCUMENTATION PAGE

Form Approved
OMB No. 0704-0188

Public reporting burden for this collection of information is estimated to average 1 hour per response, including the time for reviewing instructions, searching existing data sources, gathering and maintaining the data needed, and completing and reviewing the collection of information. Send comments regarding this burden estimate or any other aspect of this collection of information, including suggestions for reducing this burden, to Washington Headquarters Service, Directorate for Information Operations and Reports, 1216 Jefferson Davis Highway, Suite 1204, Arlington, VA 22202-4302, and to the Office of Management and Budget, Paperwork Reduction Project (0704-0188), Washington, DC 20503.

1. AGENCY USE ONLY (Leave blank)		2. REPORT DATE June 1994	3. REPORT TYPE AND DATES COVERED Final October 1992 - June 1993	
4. TITLE AND SUBTITLE A Uniaxial Nonlinear Thermoviscoelastic Constitutive Model with Damage for M30 Gun Propellant			6. FUNDING NUMBERS PR: 1L161102AH43	
6. AUTHOR(S) Geroge A. Gazonas				
7. PERFORMING ORGANIZATION NAME(S) AND ADDRESS(ES) U.S. Army Research Laboratory ATTN: AMSRL-WT-PA Aberdeen Proving Ground, MD 21005-5006			8. PERFORMING ORGANIZATION REPORT NUMBER	
9. SPONSORING/MONITORING AGENCY NAME(S) AND ADDRESS(ES) US Army Research Laboratory ATTN: AMSRL-OP-AP-L Aberdeen Proving Ground, MD 21005-5066			10. SPONSORING/MONITORING AGENCY REPORT NUMBER ARL-TR-469	
11. SUPPLEMENTARY NOTES				
12a. DISTRIBUTION/AVAILABILITY STATEMENT Approved for public release; distribution is unlimited.			12b. DISTRIBUTION CODE	
13. ABSTRACT (Maximum 200 words) The nonlinear thermoviscoelastic constitutive behavior of a conventional tank gun propellant, M30, is modeled using a modified superposition integral that incorporates the effects of microstructural fracture damage. This work represents a thermoviscoelastic extension of previous work (Gazonas 1992, 1993) that modeled the loading rate behavior of the propellant over nearly five decades in strain rate. In this work, uniaxial compression tests are conducted on the propellant at constant strain rates of .01 and 210 l/s and temperatures of -30 and 60 degrees Celsius. A master relaxation modulus is determined from the data in the form of a modified power law (MPL) in reduced time. The coefficients of the MPL are found through nonlinear inversion of the data using a Marquardt-Levenberg algorithm. Time-temperature superposition is employed and the horizontal shift function for each strain level is given by an Arrhenius expression. The propellant is nonlinearly viscoelastic since the logarithm of the vertical shift function is a quadratic function of the logarithmic strain. Theoretical predictions of time-dependent stress versus time, failure stress versus failure time and failure stress versus strain rate quantitatively agree with the experimental behavior of the propellant determined at various strain rates and temperatures.				
14. SUBJECT TERMS constitutive modeling, M30 gun propellant, nonlinear thermoviscoelasticity, continuum damage mechanics, continuum mechanics, gun propellants			15. NUMBER OF PAGES 35	
			16. PRICE CODE	
17. SECURITY CLASSIFICATION OF REPORT UNCLASSIFIED	18. SECURITY CLASSIFICATION OF THIS PAGE UNCLASSIFIED	19. SECURITY CLASSIFICATION OF ABSTRACT UNCLASSIFIED	20. LIMITATION OF ABSTRACT UL	

INTENTIONALLY LEFT BLANK.

ACKNOWLEDGMENT

Special thanks go to Mr. Michael G. Leadore for conducting the constant strain rate tests (at -30° and 60° C) on the M30 gun propellant.

INTENTIONALLY LEFT BLANK.

TABLE OF CONTENTS

	Page
ACKNOWLEDGMENT	iii
LIST OF FIGURES	vii
LIST OF TABLES	vii
1. INTRODUCTION	1
2. THE CONSTITUTIVE THEORY	4
2.1 Strain-History Inputs	6
2.2 Extension to Thermoviscoelasticity with Damage	7
3. EXPERIMENTAL RESULTS	8
4. MASTER RELAXATION MODULUS DETERMINATION	8
5. SUMMARY AND CONCLUSIONS	13
6. REFERENCES	21
DISTRIBUTION LIST	25

Accession For	
NTIS GRA&I	<input checked="" type="checkbox"/>
DTIC TAB	<input type="checkbox"/>
Unannounced	<input type="checkbox"/>
Justification	
By _____	
Distribution/ _____	
Availability Codes	
Dist	Avail and/or Special
A-1	

INTENTIONALLY LEFT BLANK.

LIST OF FIGURES

Figure		Page
1.	Uniaxial Compression of M30 Gun Propellant versus Temperature.....	16
2.	Servo-hydraulic Test Frame and Upper/Lower Piston Assembly.....	16
3.	Secant Modulus versus Reduced Time at Various Strain Levels.....	17
4.	Thermomechanical Shift Function versus $1/T$	17
5.	Vertical Shift Function versus Normalized Strain.....	18
6.	Master Relaxation Modulus (at 2% strain) versus Reduced Time.....	18
7.	Overlay of Observed (symbols) and Theoretical (solid lines) Stress versus Time Curves for M30 Gun Propellant Under Constant Strain Rate Deformation.....	19
8.	Overlay of Observed (symbols) and Theoretical (solid lines) Stress versus Time Curves for M30 Gun Propellant at Two Strain Rates (0.01 and 210 sec^{-1}) and Temperatures (-30° and 60° C).....	19
9.	Stress at Failure versus Failure Time as a Function of Temperature.....	20
10.	Stress at Failure versus Strain Rate as a Function of Temperature.....	20

LIST OF TABLES

Table		Page
1.	Chemical Composition and Nominal Specimen Dimensions of M30 Gun Propellant.....	15

INTENTIONALLY LEFT BLANK.

1. INTRODUCTION

The occurrence of high-amplitude pressure waves in guns may lead to catastrophic breech blows. Several factors that cause the pressure waves include a malfunctioning igniter, reduced charge permeability, a high initial gas generation rate, and charge compaction which results in grain fracture (May and Horst 1979; Keller and Horst 1989). Grain fracture leads to an increase in the mass burning rate of the propelling charge through an increase in the surface area available for combustion. The growth and coalescence of stress-induced microfractures alter the microstructure of gun propellant and can dramatically increase the apparent burning rate in damaged propellant relative to undamaged propellant (Gazonas et al. 1991).

The dynamics of crack growth in granular propellant are critically dependent upon the crack velocity relative to the propellant burn rate. Slowly growing microcracks that propagate as a result of intergranular stress in the propellant bed may be entirely consumed by rapid burning of the propellant grains. In some very high burn rate (VHBR) hivelite-based propellants, proposed for use in traveling charges, the apparent burning rate approaches 300 m/sec (May et al. 1984); a surface-fracturing mechanism was proposed to explain the rapid burning rates observed in VHBR propellants. The burning rates of conventional gun propellants are considerably less than in VHBR propellants. For example, the burning rates of single grains of undamaged M30 propellant are pressure-dependent and approach 10 cm/sec at 60 MPa hydrostatic pressure (Gazonas et al. 1991). Alternatively, rapidly growing microcracks that are hydraulically driven by gaseous combustion products (Wu et al. 1992; Griffiths and Nilson 1992) might accelerate the apparent burning rate through convective heating of the propellant. Cracks in many materials propagate at velocities which range from quasistatic (Atkinson and Meredith 1987) to dynamic (Swanson 1982); the upper bound on crack velocity is theoretically limited by the Rayleigh wave velocity, under usual types of loading in isotropic elastic media (Sih 1968). However, supersonic crack velocities have been observed in solids subjected to strong laser pulses (Winkler 1973) or high intensity electron beams (Cherepanov and Borzykh 1993). Shear wave speeds in low-density propellant materials are approximately 2 km/sec (Costantino 1983), which indicates that maximum crack velocities in conventional propellants are about four orders of magnitude greater than propellant burning rates.

Hence, for most interior ballistic applications that involve high-amplitude pressure wave loading of the propellant, microcrack growth rates will far exceed the burning rate of the propellant. The disparity in time scales between physical processes (crack speed and burning rate) is further exacerbated by the fact that not all regions of the granular charge are ignited simultaneously; the flamespreading rate depends upon the gas permeability of the granular propellant charge. A consideration of these observations could simplify interior ballistic numerical model development because in some instances, the mechanics problem can be temporally decoupled from the combustion problem.

However, the presence of microfractures in gun propellant is not necessarily deleterious to the mechanical, combustion, or inertability response of the propellant; it is known, for example, that distributed microcracks in certain composite materials can improve their toughness or *global* resistance to fracture. In principle then, a gun propellant could be designed to "programmably" fracture in a predictable and reproducible manner. This proposal is contrary to traditional strategies of propellant formulation that aim to minimize the fracturability of the propellant through the addition of energetic plasticizers and other ingredients. The microstructural fabric of the propellant also plays a major role in subsequent growth and coalescence of microcracks. For example, Fong and Moy (1982) suggest that propellants that contain ground spherical nitroguanidine oxidizer will have fewer possible crack propagation sites than propellants that contain long needle-like nitroguanidine crystallites. Grain size, orientation, pore size, shape and distribution, and a multitude of other structural elements that compose the microstructural fabric of the propellant will undoubtedly influence the initial distribution and subsequent growth and coalescence of microcracks. The proposed scheme recognizes that microcracks are present in nearly all manufactured materials and that the effects of microcrack growth can be predicted and therefore advantageously used in the design of new propellants.

The idea that gun performance is improved if additional surface area is introduced into the propellant charge is not new. For quite some time, ammunition designers have used multi-perforation grain design concepts to alter the mass generation rate of propellant during burning (for example, see *Military Explosives* (1955), and *Engineering Design Handbook* (1965)). Multiperforation grain designs allow for the "progressive" increase in the total surface area of the propellant grain as it burns. By mathematically modeling the progressive growth of stress-induced microfractures, one could, in

principle, design high-performance yet "safe" propellant charges *for* fracture.

An essential feature of the strategy just described is the development of a mathematical model that can predict the incremental time-dependent increase in stress-induced fracture surface area in the propellant at temperature and loading rate conditions relevant to the gun environment. Recent advances in continuum mechanics make it possible to characterize and quantify microcrack growth using concepts from the relatively new field of continuum damage mechanics (CDM). Krajcinovic (1989) provides an in-depth review of CDM from both microphysical and phenomenological standpoints. The CDM model predictions of fracture surface area could then be quantitatively compared to the progressive development of fracture surface area in the propellant derived by conducting closed bomb tests on incrementally damaged propellant. Progress with this concept began in a study that examined the effect of various mechanical variables such as strain, strain rate, and temperature on the combustion response of two conventional gun propellants (Gazonas et al. 1991). In that study, it was found that surface area evolution in M30 and JA2 gun propellants is relatively insensitive to strain rate when compared to the effects of temperature and the degree of axial deformation.

In this report, a uniaxial nonlinear thermoviscoelastic constitutive model with time-dependent damage is developed for the conventional tank gun propellant, M30. This work extends previous work that modeled loading rate behavior of the propellant over nearly five decades in strain rate (Gazonas 1992, 1993). Wave speeds in porous propellant media have been directly measured as a function of hydrostatic pressure (Costantino 1983) and estimated from propellant bed compaction studies (Kooker 1990). However, constitutive models for gun propellants are virtually nonexistent. This work represents a continuing effort to mathematically model the constitutive response of solid propellant necessary in two-phase (solid and gas) flow numerical models of interior ballistic processes. Furthermore, the work offers a means for mathematically modeling the progressive growth of microcracks that could be used in designing new propellants with the expanded "fracturable" propellant design concept described previously.

This report employs a uniaxial specialization of a general three-dimensional constitutive theory for nonlinear viscoelastic materials with damage (Schapery 1981). Herein, the previous rate-dependent model is extended to incorporate temperature effects by replacing real time variables with reduced time

variables. Theoretical predictions of time-dependent stress versus time, failure stress versus failure time, and failure stress versus strain rate quantitatively agree with the experimental behavior of the propellant determined at various strain rates and temperatures.

2. THE CONSTITUTIVE THEORY

Biot (1954) developed the unified theory of linear viscoelasticity based upon the theory of irreversible thermodynamics. Later, the theory was extended to include nonlinear thermoviscoelastic media (Schapery 1964) and distributed damage effects using a so-called "modified superposition integral" (Schapery 1981). The uniaxial strain ϵ in a material subjected to a uniaxial stress σ can be written with the notation of Schapery (1989) as,

$$\epsilon(t) = E_r \int_{0^-}^t D(t-\tau) \frac{df}{d\tau} d\tau \quad (1)$$

The integral in (1) is also known as an hereditary or convolution of the functions D and \dot{f} . The strain is thus seen to be dependent upon the entire history of application of stress and not just on the instantaneous value as in the case of nonlinearly elastic materials. It is assumed that $\epsilon = \sigma = f = 0$ when $t < 0$ and $D(t-\tau) = 0$ when $t < \tau$. Furthermore, the lower limit in the integral is 0^- to allow for a possible jump discontinuity in the function $f(t)$ at $t = 0$. All subsequent hereditary integrals appearing with the lower limit at 0 are to be interpreted as 0^- as well. D is the uniaxial creep compliance, E_r is a constant reference modulus with units of stress, and f is given as a product of two functions g_1 and $g_{2\sigma}$ as,

$$f = f(\sigma, S_{\sigma}) = g_1(\sigma) g_{2\sigma}(S_{\sigma}) \quad (2)$$

in which g_1 is typically written as a power-law function of stress and $g_{2\sigma}$ is a function of the damage

parameter. The S_{α} are k damage parameters used to describe microstructural changes that occur which alter the material's fabric. In previous work (Gazonas 1992,1993) it was shown that a single scalar damage parameter, S_{σ} , was sufficient for modeling microcrack growth in M30 gun propellant. One could argue that a one-dimensional model cannot further our understanding of three-dimensional microphysical fracture processes that occur in a propellant grain. Nevertheless, the simplification appears to be valid for describing the global constitutive behavior of M30 propellant and a variety of other materials including marine sediment, composites, polymers, rocket propellant, and ice. Regardless of the dimensionality of the proposed model, it should ultimately be reducible to a one-dimensional form that can be verified through experimentation. If a sufficient number of material tests are conducted using deformation histories similar to those experienced by the gun propellant during firing, one can develop empirical models thus circumventing the need for the development of more complex microphysical models.

The damage parameter S_{σ} in (2) is stress-history dependent and is expressed as,

$$S_{\sigma} = \int_0^t \left| \frac{\sigma}{\sigma_1} \right|^q f_1 dt , \quad (3)$$

in which σ_1 and q are positive constants, and $||$ denotes the absolute value of the quantity. The "crack tip material-related coefficient" f_1 can depend on time and temperature and material aging effects (Schapery 1981,1989). For example, extension of the isothermal theory to account for transient temperature effects involves replacing f_1 in (3) by the factor $(1/a_T)$ and using reduced time in Eqns. (1) through (3). The thermomechanical shift factor, a_T , is related to entropy production in Schapery's thermodynamic theory. The extension of the model to incorporate thermoviscoelastic behavior of the propellant is provided in a subsequent section.

The underlying physical basis for the constitutive theory with distributed damage is a crack growth "law" that relates the speed \dot{a} of a single crack to a power-law function of the mode I stress

intensity factor, $\dot{a} = A K_I^Q$, in which A and Q are empirically determined constants. Schapery (1975) arrives at this result by generalizing Barenblatt's (1962) cohesive crack tip model for linear elastic media to linearly viscoelastic media. The crack propagation theory is later generalized (Schapery 1981, 1984) to encompass nonlinear viscoelastic behavior through the use of the so-called "pseudo-variables." The use of pseudo-variables for describing damage effects in nonlinearly viscoelastic media effectively reduces the problem to one of nonlinear elasticity since stress-pseudostrain plots are single-valued (Schapery 1982). In an analogous fashion, a pseudostress transformation could be invoked to create a single-valued curve in worksoftening materials.

A complete derivation that extends the single-crack theory to describe the global response of the medium due to distributed microcracking is beyond the scope of this report but is addressed in Schapery (1981) (Equations 122 through 126). The derivation uses a relation between crack speed and a power-law function of a generalized J-integral (Schapery 1981, 1984).

2.1 Strain-History Inputs. Equations (1) through (3) are suitable for characterizing a material's strain response if stress is a controlled input for the test. However, if strain is a controlled input for the test, then these equations can be inverted to predict stress as a function of strain history,

$$\sigma(t) = \sigma_2 \epsilon^{\circ 1/t} g_{2\epsilon}(S_2) \operatorname{sgn}(\epsilon^{\circ}) , \quad (4)$$

in which sgn is the signum function, σ_2 is a constant parameter with units of stress, $g_{2\epsilon}(S_2) = g_{2\sigma}(S_{\sigma})^{-1/t}$ (Schapery 1989), and the pseudo-strain, ϵ° , is related to strain history by,

$$\epsilon^{\circ} = E_T^{-1} \int_0^t E(t-\tau) \frac{d\epsilon}{d\tau} d\tau , \quad (5)$$

in which $E(t)$ is the relaxation modulus. A damage parameter S_e for strain history inputs (Schapery 1989) is

$$S_e = (\sigma_2/\sigma_1)^q \int_0^t e^{-q\sigma_1 t} f_1 dt \quad (6)$$

in which σ_2 , σ_1 , q , and r are material-dependent constants.

2.2 Extension to Thermoviscoelasticity with Damage. The extension of the model to incorporate thermoviscoelasticity with damage is performed by replacing the time variable t with a reduced time variable ξ in the previous equations. Furthermore, determination of the master relaxation modulus $E(\xi)$ is traditionally obtained by performing stress-relaxation tests at various temperatures and then rigidly shifting the time scales for each of the tests to form a continuous, single-valued curve (Morland and Lee 1960). The single-valued curve then represents the relaxation modulus, (or creep compliance if a unit Heaviside stress-history is applied) at the reference temperature, for very short, intermediate, and very long times. If the master relaxation modulus can be formed through horizontal translations of the data, the material is termed thermorheologically simple. The master relaxation modulus is plotted as a function of a reduced time parameter ξ defined by,

$$\xi = \int_0^t \frac{dt}{a_T(e, T)} \quad (7)$$

in which a_T is the thermomechanical shift function defined as $a_T = 1$ at the reference temperature. The prediction of time-dependent stress in (4) is then made by replacing real time in (5) with reduced time, which yields for the pseudostrain,

$$e^p = E_r^{-1} \int_0^t E(\xi - \xi') \frac{d\xi}{d\tau} d\tau \quad (8)$$

$E(\xi)$ in (8) is traditionally determined by conducting uniaxial stress-relaxation tests. In a subsequent section, it is shown how constant strain rate compression tests, conducted at various temperatures, can be used to determine $E(\xi)$.

3. EXPERIMENTAL RESULTS

Experimental results for isothermal uniaxial compression of M30 propellant at two strain rates, 0.01 and 210 sec^{-1} , and three temperatures, -30° , 21° , and 60° C appear in Figure 1. Each stress-time curve is a composite curve formed from the average of five tests. The uniaxial compression tests are performed using an MTS high rate 810 material test system described in more detail elsewhere (Gazonas 1991). The maximum piston velocity is approximately 12 m/sec, which limits the axial compressive strain rate to 500 sec^{-1} on 25-mm specimens. Constant strain rate tests are performed by computer control of the piston velocity through feedback from an externally mounted linear-variable differential transformer (LVDT, MTS Model 244.11). Force is measured with a 60-kN quartz-piezoelectric force transducer (Kistler Type 9031A) that is mounted on the upper moving piston (Figure 2). Specimen displacements are corrected for apparatus distortion that has a measured stiffness of about 92 kN/mm. Specimen stiffness ranges from 4.5 to 14 kN/mm at room temperature for the strain rate range investigated. Specimens are thermally conditioned at temperature for about 1 hour before testing in a Thermotron conditioning oven/refrigerator (Controller Model 5200) that houses both upper and lower pistons. The chemical composition and nominal specimen dimensions of M30 appear in Table 1.

4. MASTER RELAXATION MODULUS DETERMINATION

The master relaxation modulus is experimentally determined using the results of constant strain rate tests conducted at -30° , 21° , and 60° C. In earlier work, it was shown that the relaxation modulus for M30, JA2, and XM39 propellants is derivable from constant strain rate test data (Gazonas 1991). For a constant strain rate test, the one-dimensional linear viscoelastic constitutive equation without damage is written as,

$$\sigma(t) = \int_0^t E(t-\tau) \frac{d\varepsilon}{d\tau} d\tau . \quad (9)$$

For a constant strain rate input history, i.e., $\varepsilon = \dot{\varepsilon} t$, (9) becomes,

$$\sigma(t) = \dot{\varepsilon} \int_0^t E(t-\tau) d\tau . \quad (10)$$

The secant modulus is defined as,

$$E_s = \frac{\sigma}{\varepsilon} , \quad (11)$$

and since $\varepsilon = \dot{\varepsilon} t$,

$$E_s = t^{-1} \int_0^t E(u) du . \quad (12)$$

Taking derivatives of both sides of (12) results in an expression for the relaxation modulus,

$$E(t) = E_s + t \frac{dE_s}{dt} . \quad (13)$$

Equation (13) can be rewritten as

$$E(t) = E_s \left(1 + \frac{dE_s}{dt} \frac{t}{E_s} \right) . \quad (14)$$

Using a property of logarithms (i.e., $\ln_{10} d(\log_{10} x) = dx/x$, (14) can be rewritten as,

$$E(t) = E_s \left(1 + \frac{d \log_{10} E_s}{d \log_{10} t} \right). \quad (15)$$

If the slope of the $\log_{10} E_s$ versus $\log_{10} t$ curve is much less than unity, then the relaxation modulus is essentially equivalent to the secant modulus. To determine if the relaxation modulus of M30 is nonlinear (strain dependent), one can plot the secant modulus σ/ϵ at strain levels of 2, 5, 10, 15, 20, 25, 30, and 35% versus reduced time ξ (Figure 3).

If the thermomechanical shift function a_T depends primarily on temperature and not on strain level in (7), then $a_T = a_T(T)$. Furthermore, if temperature is timewise constant, Equation (7) reduces to $\xi = t/a_T$; the effects of transient temperature changes in the gun environment may be negligible relative to effects of the propagation of mechanical disturbances (P and S waves). The thermomechanical shift function is described by an Arrhenius expression,

$$\log_{10} a_T = \left(\frac{Q}{2.303 R} \right) \left[\frac{1}{T} - \frac{1}{T_r} \right], \quad (16)$$

in which Q is the activation energy (kcal/mole), R is the universal gas constant (1.987 cal/g-mole K), and T_r is the reference temperature (K). The activation energy is 27.4 kcal/mole determined from the slope of the $\log_{10}(a_T)$ versus $1/T$ curve since $d(\log_{10}(a_T))/d(1/T) = Q/2.303R$ (Figure 4). Although the data are limited, it appears that the thermomechanical shift function exhibits some strain dependence. The amount of strain-dependent shift is greater at -30°C than at 60°C (Figure 4). From the stress relaxation data of Lieb and Leadore (1992), an activation energy of 29.6 kcal/mole is derived that is only 8% greater than the activation energy reported herein; the difference in the calculated activation energy may also be attributed to the fact that the stress relaxation experiments of Lieb and Leadore (1992) are conducted on a different lot of multiperforated M30 propellant, whereas the test results reported herein are conducted on solid stick M30 propellant.

Since the material is nonlinearly viscoelastic, a vertical shift function, a_v , is used to collapse the relaxation moduli determined at each strain level (Figure 3) onto a single master curve. The logarithm of the vertical shift function is empirically determined to be a quadratic function of the logarithm of strain (Figure 5). The amount of vertical shift is unity when the strain level ϵ equals the reference strain level ϵ_r of 2%. Figure 6 illustrates an overlay of the data and the master relaxation modulus (at 2% strain) which takes the form of a modified power-law (MPL) in reduced time; the coefficients of the MPL are determined using a nonlinear least squares inversion technique (Marquardt-Levenberg algorithm). The MPL is written as,

$$E(\xi) = E_{\infty} + \frac{(E_0 - E_{\infty})}{(1 + \frac{\xi}{t_0})^n}, \quad (17)$$

in which $E_0 = E(0^+)$ and $E_{\infty} = E(\infty)$ are the short-term and long-term asymptotes of the relaxation modulus, and t_0 and n are additional free constants. The constants assume values, $E_0 = 4,470 \pm 628$ MPa, $E_{\infty} = 453 \pm 94$ MPa, $n = 0.171 \pm .031$, and $t_0 = 4.6 \times 10^{-6} \pm 6.2 \times 10^{-6}$ secs. Equation (17) increases the range of behavior of M30 over a broad time spectrum. For example, if the propellant is strained to 2% at room temperature, the secant modulus relaxes from 4,470 MPa to 453 MPa (about an order of magnitude) in about 28 hours. The same relaxation requires about 1.6 minutes at 60° C and about 6.4 years at -30° C.

Substitution of the relaxation modulus $E(\xi)$ into (8) and then substitution of the pseudostrain into (6) and (4) completes the extension of the model to thermoviscoelasticity. If the theory is correct, the form of the damage function $g_{2\epsilon}(S_{\epsilon}) = 10^{-1.5(1 - \sqrt{1 - \xi^2})}$ is identical to that determined previously for M30 (Gazonas 1991,1992), in which $\xi = \log_{10}(S_{\epsilon})/\log_{10}(S_{\text{max}})$. The assumption is that all temperature effects are introduced into the damage function $g_{2\epsilon}(S_{\epsilon})$ and damage parameter S_{ϵ} through the pseudostrain in (8) which is a function of temperature-reduced time.

How well the model fits the data for a particular material will depend upon whether a single scalar

damage parameter adequately accounts for damage evolution throughout the range in test temperatures. Previous work accurately modeled loading rate effects (over nearly five decades in strain rate) in M30 with a single, scalar damage parameter (Figure 7). In general, multiple damage parameters are specified using (2); a damage-reduced time shift function approach might also be employed to account for more complex temperature-dependent behavior.

The current model is further simplified if a power-law relaxation modulus (Gazonas 1992, 1993),

$$E(t) = E_1 t^{-n} \quad (18)$$

is used rather than the MPL relaxation modulus in (17). Replacing real time with reduced time in (18) and then substituting (18) into (8) with $\xi = t/a_T$, $E_1 = E_r$, and for a constant strain rate input history, $\epsilon = \dot{\epsilon} t$, yields an expression for the pseudostrain,

$$\epsilon^o(t) = a_T^n \dot{\epsilon} \frac{t^{1-n}}{n+1} \quad (19)$$

Substitution of (19) into (6) with $f_1 = (1/a_T)$ and $\sigma_1 = \sigma_2 \dot{\epsilon}_{ref}^{1/n}$ yields for the damage parameter,

$$S_e(t) = \left[\frac{\epsilon^o}{\dot{\epsilon}_{ref}} \right]^{q/r} \frac{t}{a_T} \frac{1}{(1-n)\frac{q}{r} + 1} \quad (20)$$

Time-dependent stress (Figure 7) is predicted by substituting (19) and (20) into (4) using the ellipsoidal damage function $g_{ze}(S_e)$ and constants determined previously (Gazonas 1992, 1993). Model predictions of time-dependent stress agree fairly well with the experimental data (Figure 8).

The failure stress (maximum stress) in M30 propellant decreases as both failure time (time

required to reach maximum stress) and temperature increases. The coefficient of the power law relation is about - 0.10 for tests conducted at -30°, 21°, and 60° C (Figure 9). The failure stress at a given temperature increases by a factor ranging from 2 to 3 over nearly five decades in strain rate. Furthermore, the mechanical behavior of M30 is dominated by temperature changes since the failure stress at a given strain rate also increases by a factor ranging from 2 to 3 when the temperature increases from 21° C to 60° C; equivalent changes in the magnitude of the failure stress in the propellant are seen by changing strain rate by nearly five orders of magnitude. Failure strains are seen to increase slightly with temperature; however at a given temperature, failure strains are insensitive to strain rate. This is seen by substituting the power-law expression for failure time and strain rate (Figures 9 and 10) into the expression, $\epsilon_f = t_f \dot{\epsilon}$, and recognizing that the result is a constant.

5. SUMMARY AND CONCLUSIONS

A nonlinear theory of viscoelasticity with damage (Schapery 1981) has been extended to account for the effects of both temperature (-30° to 60° C) and strain rate (10^{-2} sec^{-1} to 400 sec^{-1}) on the constitutive response of M30 gun propellant. Theoretical time-dependent stresses in the propellant subjected to a timewise constant temperature field and arbitrary input strain-history are obtained by replacing real time variables with reduced time variables. The theoretical predictions of time-dependent stress versus time, failure stress versus failure time, and failure stress versus strain rate quantitatively agree with the experimental behavior of the propellant determined at various strain rates and temperatures.

The thermomechanical shift function for M30 propellant is determined by shifting data derived from uniaxial constant strain rate compression tests. The shift function follows an Arrhenius law with an activation energy of approximately 27.4 kcal/mole. This value compares well with an activation energy of 29.6 kcal/mole derived directly from the stress relaxation test results of Lieb and Leadore (1992).

The relaxation modulus of M30 propellant is nonlinear (strain dependent), and the logarithm of the vertical shift function is a quadratic function of the logarithmic strain. The relaxation modulus for M30 propellant has been obtained in the form of a modified power-law in reduced time; the coefficients

of the MPL are found through nonlinear inversion of the data using a Marquardt-Levenberg algorithm. However, the analysis becomes somewhat simplified using power-law form for the relaxation modulus determined in earlier work (Gazonas 1992, 1993) and incorporating all nonlinearities and damage in the function $f(\sigma, S_{\sigma})$ (Equation 2).

The effects of temperature dominate strain rate effects in M30 propellant as the magnitude of the failure stress (maximum stress) is equally affected by a change in temperature from 21° to 60° C (or 21° to -30° C) or by a change in strain rate that spans nearly five orders of magnitude. The master curve is also significant since measurements made at laboratory experiment time scales are extrapolatable to very short or very long times. For example, if the propellant is strained to 2% at room temperature, the secant modulus relaxes from 4,470 MPa to 453 MPa (about an order of magnitude) in about 28 hours. The same relaxation requires about 1.6 minutes at 60° C and about 6.4 years at -30° C. Most interior ballistic applications require extrapolation of material properties to very short times, on the order of milliseconds. The model developed herein, however, is also useful for extrapolating material properties and constitutive behavior to very long times and could be useful in the long-term design of storage facilities for propellants. Other factors such as the effects of humidity and aging effects of gun propellants are also important, but not well understood, and require further testing to aid in model development and validation.

**Table 1. Chemical Composition and Nominal Specimen Dimensions
of M30 Gun Propellant**

Component	%
Nitrocellulose 12.6 % NC Nitration	28.0
Nitroglycerin	22.0
Nitroguanidine	48.0
Ethyl Centralite	2.0
	100.0
Length (mm)	25.4
Diameter (mm)	12.3

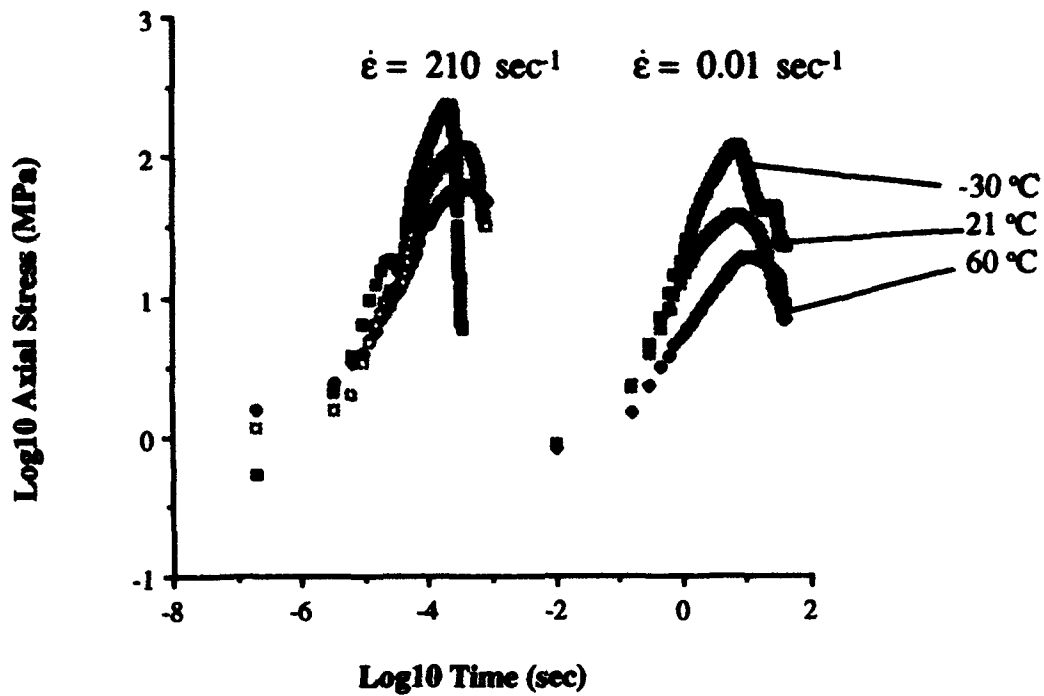


Figure 1. Uniaxial Compression of M30 Gun Propellant versus Temperature and Strain Rate.

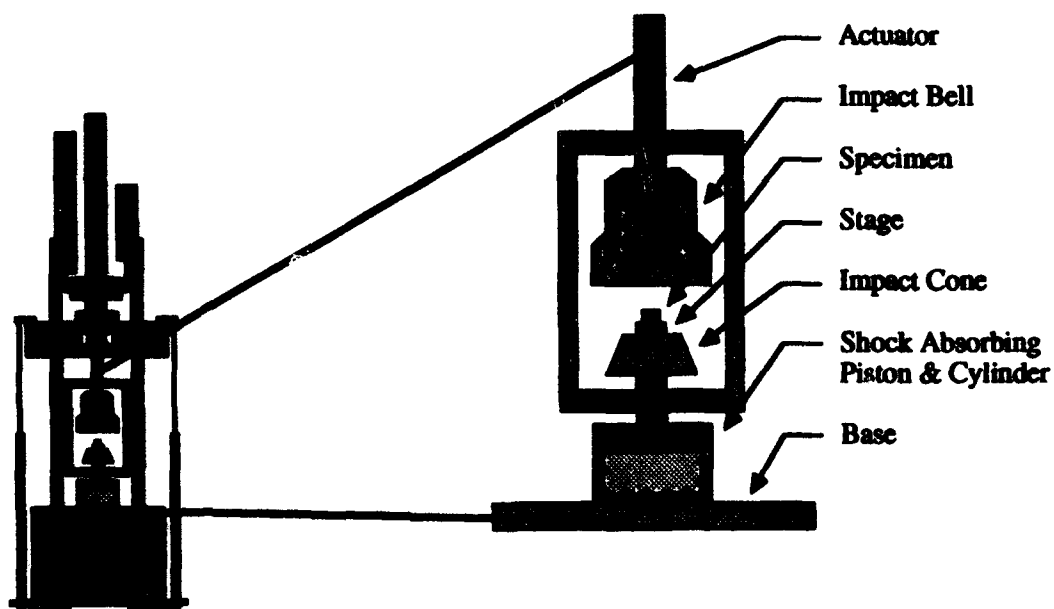


Figure 2. Servohydraulic Test Frame and Upper/Lower Piston Assembly.

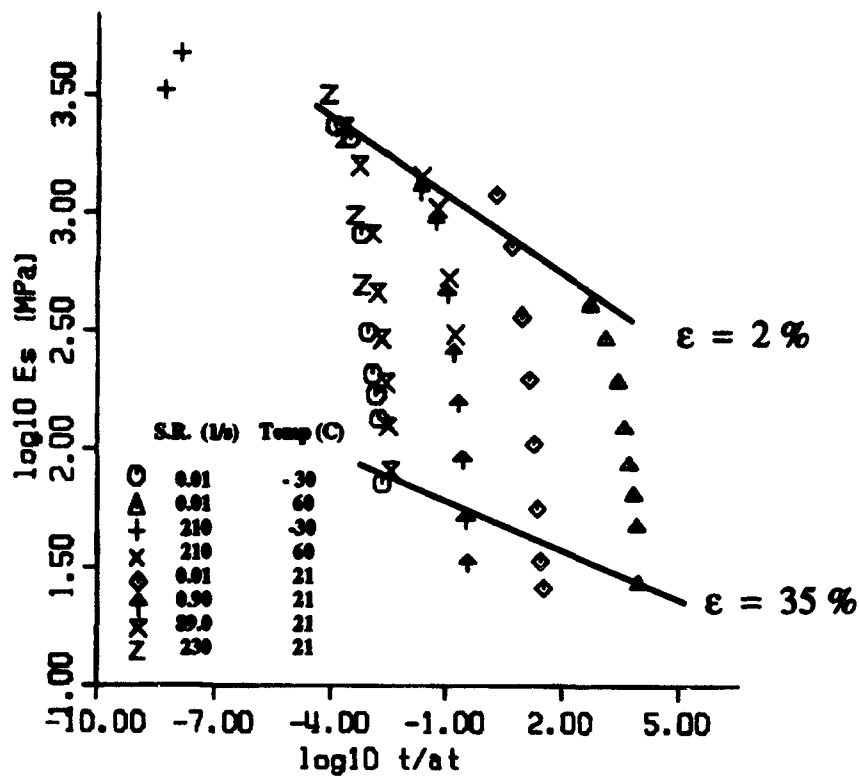


Figure 3. Secant Modulus versus Reduced Time at Various Strain Levels.

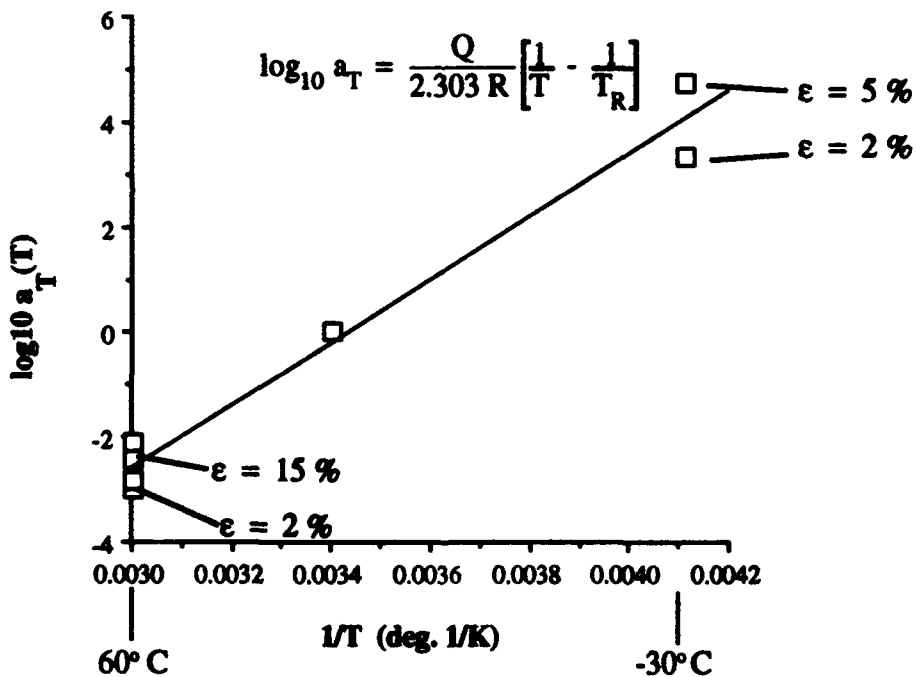


Figure 4. Thermomechanical Shift Function versus 1/T

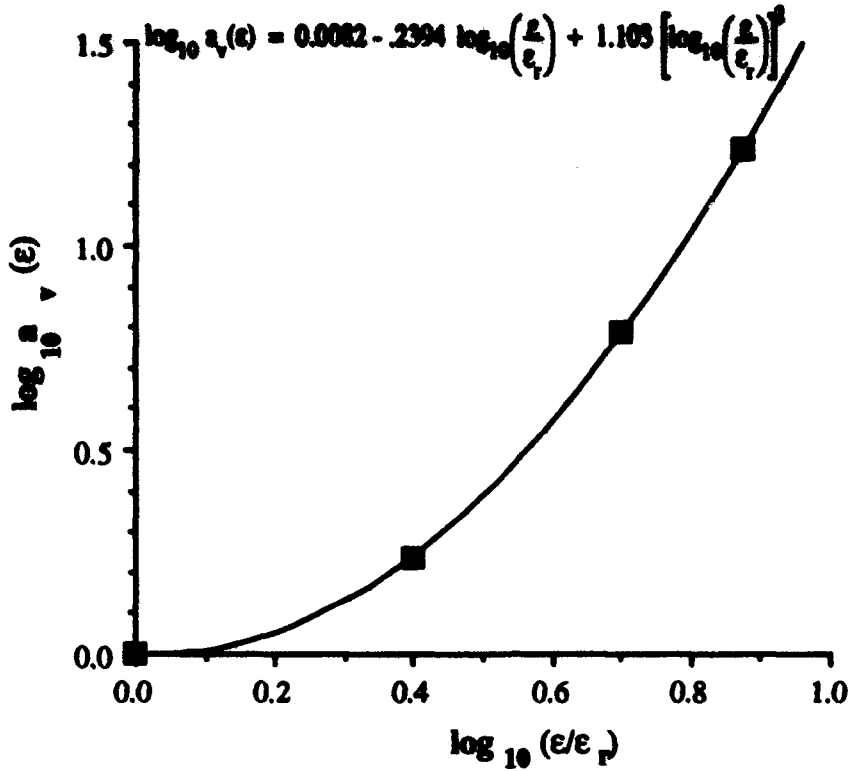


Figure 5. Vertical Shift Function versus Normalized Strain.

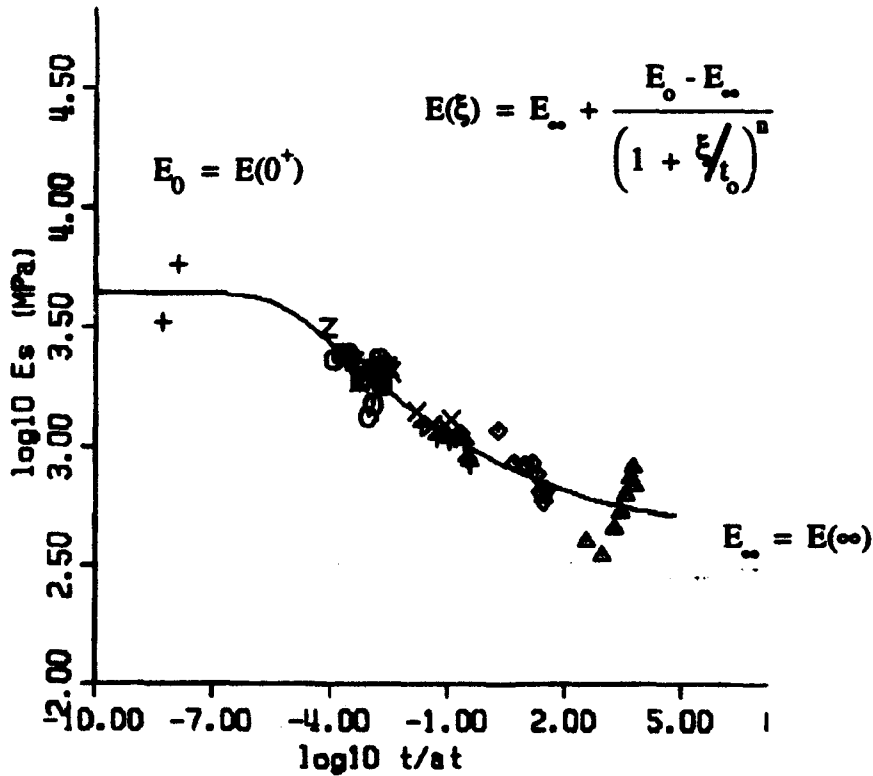


Figure 6. Master Relaxation Modulus (at 2% strain) versus Reduced Time.

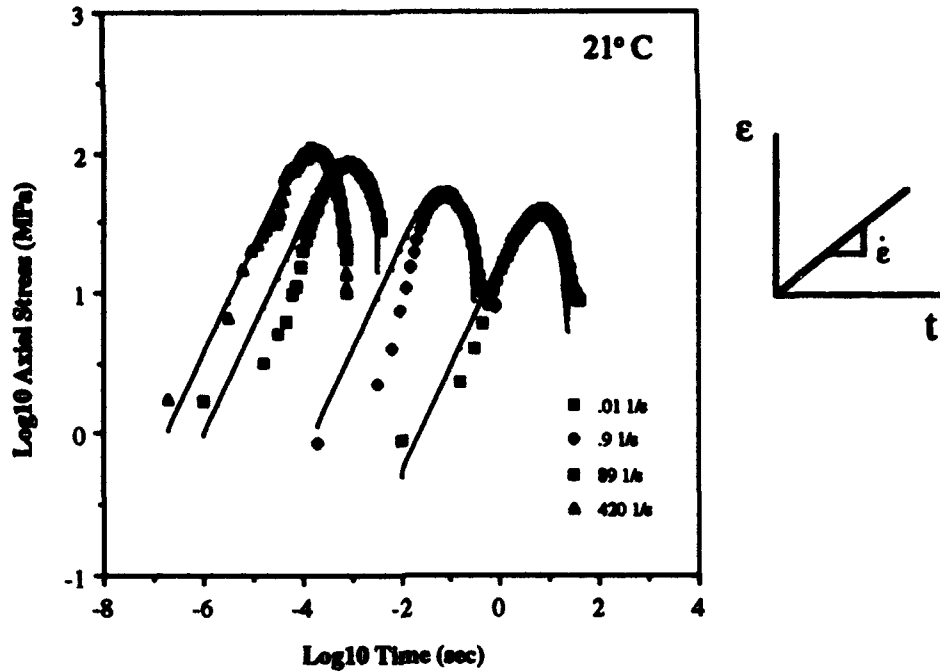


Figure 7. Overlay of Observed (symbols) and Theoretical (solid lines) Stress versus Time Curves for M30 Gun Propellant Under Constant Strain Rate Deformation.

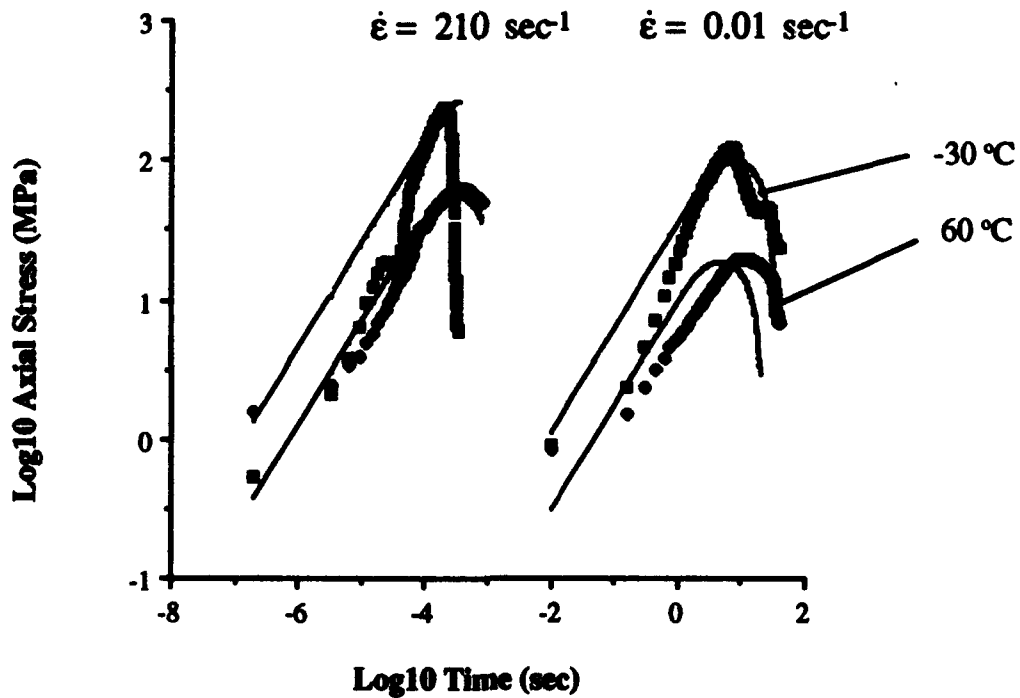


Figure 8. Overlay of Observed (symbols) and Theoretical (solid lines) Stress versus Time Curves for M30 Gun Propellant at Two Strain Rates (0.01 and 210 sec⁻¹) and Temperatures (-30° and 60°).

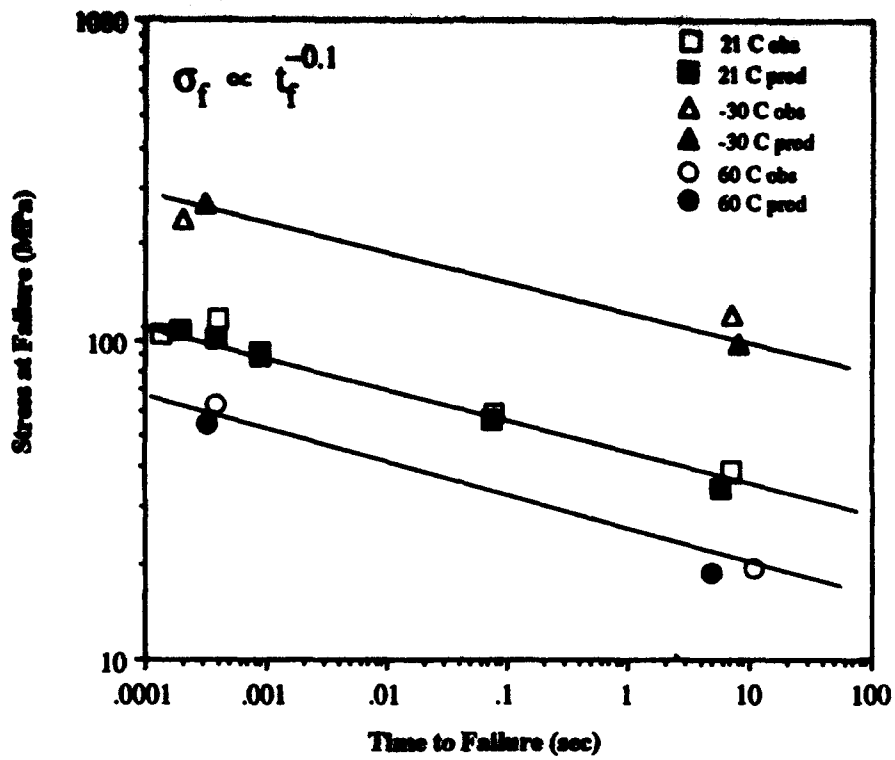


Figure 9. Stress at Failure versus Failure Time as a Function of Temperature.

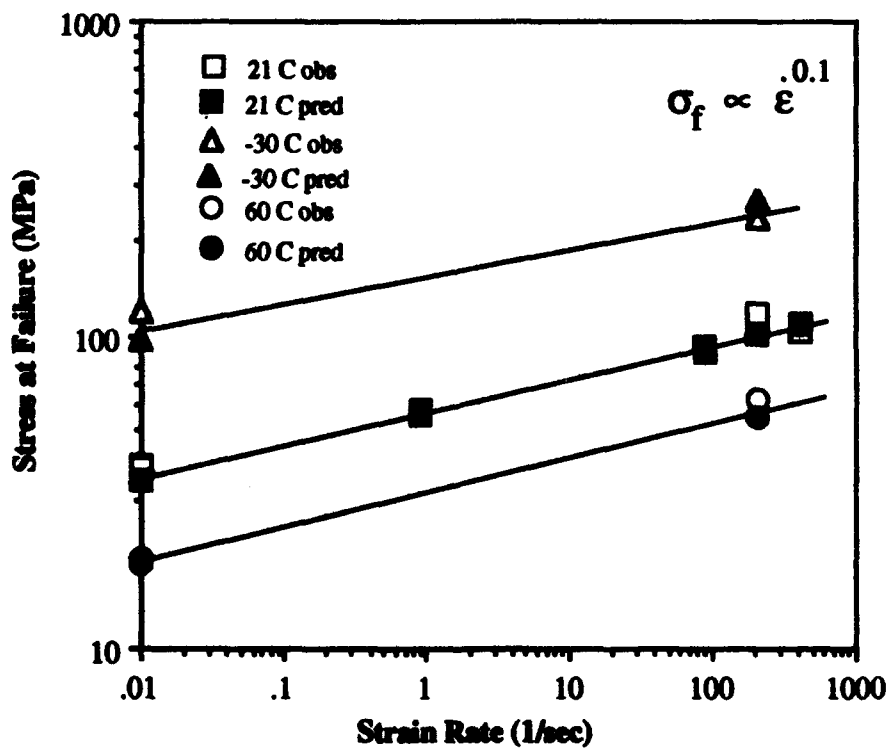


Figure 10. Stress at Failure versus Strain Rate as a Function of Temperature.

6. REFERENCES

- Atkinson, B.K., and P.G. Meredith. "The Theory of Subcritical Crack Growth with Applications to Minerals and Rocks." in: Fracture Mechanics of Rock, Edited by B.K. Atkinson, London, Academic Press, Inc., pp. 111-166, 1987.
- Barenblatt, G.I. "The Mathematical Theory of Equilibrium Cracks in Brittle Fracture." in: Advances in Applied Mechanics, Vol. VII, Academic Press, NY, pp. 55-129, 1962.
- Biot, M.A. "Theory of Stress-Strain Relations in Anisotropic Viscoelasticity and Relaxation Phenomena." J. of Appl. Phys., Vol. 25, No. 11, pp. 1385-1391, 1954.
- Cherepanov, G.P., and A.A. Borzykh. "Brittle Fracture of Solids Caused by Intense Electron Beams." Engng. Fracture Mech., Vol. 46, No. 6, pp. 1059-1088, 1993.
- Costantino, M. "Volumes and Sound Speeds of Two Gun Propellants at High Pressure." Lawrence Livermore National Laboratory, UCRL-88521, 1983.
- Engineering Design Handbook, Ballistics Series, Interior Ballistics of Guns, AMCP 706-150, U.S. Army Materiel Command, Washington, D.C., 1965.
- Fong, C.W., and B.K. Moy. "Ballistic Criteria for Propellant Grain Fracture in the GAU-8/A 30 MM Gun." AFATL-TR-82-21, Air Force Armament Laboratory, Eglin Air Force Base, FL, 1982.
- Gazonas, G.A. "The Mechanical Response of M30, XM39, and JA2 Propellants at Strain Rates from 10^{-2} to 250 sec^{-1} ." BRL-TR-3181, U.S. Army Ballistic Research Laboratory, Aberdeen Proving Ground, MD, 1991.
- Gazonas, G.A., A.A. Juhasz, and J.C. Ford. "Strain Rate Insensitivity of Damage-Induced Surface Area in M30 and JA2 Gun Propellants." BRL-TR-3251, U.S. Army Ballistic Research Laboratory, Aberdeen Proving Ground, MD, 1991.
- Gazonas, G.A. "A Uniaxial Nonlinear Viscoelastic Constitutive Model with Damage for M30 Gun Propellant." CPIA Publication 582, Vol. I, April 1992, 1992 JANNAF Propulsion Systems Hazards Subcommittee Meeting, Naval Surface Warfare Center, Silver Spring, MD, pp. 475-487, 1992.
- Gazonas, G.A. "A Uniaxial Nonlinear Viscoelastic Constitutive Model with Damage for M30 Gun Propellant." Mechanics of Materials, Vol. 15, pp. 323-335, 1993.
- Griffiths, S.K., and R.H. Nilson. "Similarity Analysis of Fracture Growth and Flame Spread in Deformable Solid Propellants." Combustion and Flame, Vol. 88, pp. 369-383, 1992.

Keller, G.E., and A.W. Horst. "The Effects of Propellant Grain Fracture on the Interior Ballistics of Guns." BRL-MR-3766, U.S. Army Ballistic Research Laboratory, Aberdeen Proving Ground, MD, 1989.

Kooker, D.E. "Modeling of Compaction Wave Behavior in Confined Granular Energetic Material." BRL-TR-3138, U.S. Army Ballistic Research Laboratory, Aberdeen Proving Ground, MD, 1990.

Krajcinovic, D. "Damage Mechanics." Mechanics of Materials, Vol. 8, pp. 117-197, 1989.

Lieb, R.J., and M.G. Leadore. "Time-Temperature Shift Factors for Gun Propellant." CPIA Publication 582, Volume I, April 1992, 1992 IANNAF Propulsion Systems Hazards Subcommittee Meeting, Naval Surface Warfare Center, Silver Spring, MD, pp. 145-151, 1992.

May, I.W., and A.W. Horst. "Charge Design Considerations and Their Effect on Pressure Waves in Guns." in: Interior Ballistics of Guns, Vol. 66, Progress in Astronautics and Aeronautics, H. Krier and M. Summerfield, Editors, pp. 197-227, 1979.

May, I.W., F.R. Lynn, A.A. Juhasz, E. Fisher, and P.S. Gough. "Thrust Characterization of Very High Burning Rate Propellants." ARBRL-MR-03359, U.S. Army Ballistic Research Laboratory, Aberdeen Proving Ground, MD, 1984.

Military Explosives Departments of the Army and the Air Force Technical Manual No. 9-1910, Technical Order No. 11A-1-34, U.S. Government Printing Office, Washington, D.C., 1955.

Morland, L.W., and E.H. Lee. "Stress Analysis for Linear Viscoelastic Materials with Temperature Variation." Trans. of the Society of Rheology, Vol. 4, pp. 233-263, 1960.

Schapery, R.A. "Application of Thermodynamics to Thermomechanical, Fracture and Birefringent Phenomena in Viscoelastic Media." J. of Appl. Phys., Vol. 35, No. 5, pp. 1451-1465, 1964.

Schapery, R.A. "A Theory of Crack Initiation and Growth in Viscoelastic Media I, II, and III." Int. J. of Fracture, Vol. 11, pp. 141-159, 369-388, and 549-562, 1975.

Schapery, R.A. "On Viscoelastic Deformation and Failure Behavior of Composite Materials with Distributed Flaws." 1981 Advances in Aerospace Structures and Materials, ASME, AD-01, Edited by S.S. Wang and W.L. Renton, New York, NY, pp. 5-20, 1981.

Schapery, R.A. "Models for Damage Growth and Fracture in Nonlinear Viscoelastic Particulate Composites." Proceedings of the Ninth U.S. National Congress of Applied Mechanics, ASME, pp. 237-245, 1982.

Schapery, R.A. "Correspondence Principles and a Generalized J Integral for Large Deformation Fracture Analysis of Viscoelastic Media." International Journal of Fracture, Vol. 25, pp. 195-223, 1984.

- Schapery, R.A. "Models for the Deformation of Viscoelastic Media with Distributed Damage and their Applicability to Ice." Proceedings of the IUTAM/IAHR Symposium on Ice/Structure Interaction, Memorial University of Newfoundland, St. John's, 1989.
- Sih, G.C. "Some Elastodynamic Problems of Cracks." Int. J. Fract. Mech. Vol. 4, pp. 51-68, 1968.
- Swanson, S.R. "Crack Velocity Measurements in Solithane 113." University of Utah Report, UTBC ME 82-004, 1982.
- Winkler, S.R. "Supersonic Crack Propagation in Ionic Crystals Induced by Strong Laser Pulses." in: Dynamic Crack Propagation, Edited by G. Sih, Noordhoff, Leyden, pp. 623-629, 1973.
- Wu, S.R., Y.C. Lu, K.K. Kuo, V. Yang, and W. Fabanich. "Combustion-Induced Crack/Debond Propagation in High-Elongation Propellants." CPIA Publication 582, Vol. I, April 1992, 1992 JANNAF Propulsion Systems Hazards Subcommittee Meeting, Naval Surface Warfare Center, Silver Spring, MD, pp. 437-451, 1992.

INTENTIONALLY LEFT BLANK.

<u>No. of Copies</u>	<u>Organization</u>	<u>No. of Copies</u>	<u>Organization</u>
2	Administrator Defense Technical Info Center ATTN: DTIC-DDA Cameron Station Alexandria, VA 22304-6145	1	Commander U.S. Army Missile Command ATTN: AMSMI-RD-CS-R (DOC) Redstone Arsenal, AL 35898-5010
1	Commander U.S. Army Materiel Command ATTN: AMCAM 5001 Eisenhower Ave. Alexandria, VA 22333-0001	1	Commander U.S. Army Tank-Automotive Command ATTN: AMSTA-JSK (Armor Eng. Br.) Warren, MI 48397-5000
1	Director U.S. Army Research Laboratory ATTN: AMSRL-OP-CI-AD, Tech Publishing 2800 Powder Mill Rd. Adelphi, MD 20783-1145	1	Director U.S. Army TRADOC Analysis Command ATTN: ATRC-WSR White Sands Missile Range, NM 88002-5502
1	Director U.S. Army Research Laboratory ATTN: AMSRL-OP-CI-AD, Records Management 2800 Powder Mill Rd. Adelphi, MD 20783-1145	(Class. only) 1	Commandant U.S. Army Infantry School ATTN: ATSH-CD (Security Mgr.) Fort Benning, GA 31905-5660
2	Commander U.S. Army Armament Research, Development, and Engineering Center ATTN: SMCAR-TDC Picatinny Arsenal, NJ 07806-5000	(Unclass. only) 1	Commandant U.S. Army Infantry School ATTN: ATSH-WCB-O Fort Benning, GA 31905-5000
1	Director Benet Weapons Laboratory U.S. Army Armament Research, Development, and Engineering Center ATTN: SMCAR-CCB-TL Watervliet, NY 12189-4050	1	WL/MNOI Eglin AFB, FL 32542-5000 <u>Aberdeen Proving Ground</u>
1	Director U.S. Army Advanced Systems Research and Analysis Office (ATCOM) ATTN: AMSAT-R-NR, M/S 219-1 Ames Research Center Moffett Field, CA 94035-1000	2	Dir, USAMSAA ATTN: AMXSY-D AMXSY-MP, H. Cohen
		1	Cdr, USATECOM ATTN: AMSTE-TC
		1	Dir, USAERDEC ATTN: SCBRD-RT
		1	Cdr, USACBDCOM ATTN: AMSCB-CII
		1	Dir, USARL ATTN: AMSRL-SL-I
		5	Dir, USARL ATTN: AMSRL-OP-AP-L

<u>No. of Copies</u>	<u>Organization</u>
1	HQDA (SARD-TR/Dr. R. Chait) Washington, DC 20310-0103
1	HQDA (SARD-TR/Ms. K. Kominos) Washington, DC 201310-0103
1	Director U.S. Army Research Laboratory ATTN: AMSRL-CP-CA, D. Snider 2800 Powder Mill Road Adelphi, MD 20783
6	Director U.S. Army Research Laboratory ATTN: AMSRL-MA-P, L. Johnson B. Halpin T. Chou AMSRL-MA-PA, D. Granville W. Haskell AMSRL-MA-MA, G. Hagnauer Watertown, MA 02172-0001
4	Commander U.S. Army Armament Research, Development, and Engineering Center ATTN: SMCAR-FSE, T. Gora E. Andricopoulos B. Knutelsky A. Graf Picatinny Arsenal, NJ 07806-5000
3	Commander U.S. Army Armament Research, Development, and Engineering Center ATTN: SMCAR-TD, R. Price V. Linder T. Davidson Picatinny Arsenal, NJ 07806-5000
1	Commander U.S. Army Armament Research and Development Center ATTN: F. McLaughlin Picatinny Arsenal, NJ 07806

<u>No. of Copies</u>	<u>Organization</u>
5	Commander U.S. Army Armament Research, Development, and Engineering Center ATTN: SMCAR-CCH-T, S. Musalli P. Christian K. Fehsal N. Krasnow R. Carr Picatinny Arsenal, NJ 07806-5000
1	Commander U.S. Army Armament Research, Development, and Engineering Center ATTN: SMCAR-CCH-V, E. Fennell Picatinny Arsenal, NJ 07806-5000
1	Commander U.S. Army Armament Research, Development, and Engineering Center ATTN: SMCAR-CCH, J. DeLorenzo Picatinny Arsenal, NJ 07806-5000
2	Commander U.S. Army Armament Research, Development, and Engineering Center ATTN: SMCAR-CC, J. Hedderich Col. Sinclair Picatinny Arsenal, NJ 07806-5000
1	Commander U.S. Army Armament Research, Development, and Engineering Center ATTN: SMCAR-CCH-P, J. Lutz Picatinny Arsenal, NJ 07806-5000
2	Commander U.S. Army Armament Research, Development, and Engineering Center ATTN: SMCAR-FSA-M, D. DeMella F. Diorio Picatinny Arsenal, NJ 07806-5000
1	Commander U.S. Army Armament Research, Development, and Engineering Center SMCAR-FSA, C. Spinelli Picatinny Arsenal, NJ 07806-5000

<u>No. of</u> <u>Copies</u>	<u>Organization</u>
11	<p>Director Beast Laboratories ATTN: SMCAR-CCB, C. Kitchens J. Keane T. Allen J. Vasilakis G. Friar T. Simkins V. Montvori J. Wrzochalski G. D'Andrea R. Hasenbein SMCAR-CCB-R, S. Sopok Watervliet, NY 12189</p>
1	<p>Commander ATTN: SMCWV-QAE-Q, C. Howd Bldg 44 Watervliet Arsenal Watervliet, NY 12189-4050</p>
1	<p>Commander ATTN: SMCWV-SPM, T. McCloskey Bldg 25/3, Watervliet Arsenal Watervliet, NY 12189-4050</p>
1	<p>Commander Watervliet Arsenal ATTN: SMCWV-QA-QS, K. Insko Watervliet, NY 12189-4050</p>
1	<p>Commander Production Base Modernization Activity U.S. Army Armament Research, Development, and Engineering Center ATTN: AMSMC-PBM-K Picatinny Arsenal, NJ 07806-5000</p>
1	<p>Commander U.S. Army Belvoir RD&E Center ATTN: STRBE-JBC, C. Kominos Fort Belvoir, VA 22060-5606</p>
1	<p>U.S. Army Cold Regions Research and Engineering Laboratory ATTN: P. Dutta 72 Lyme Road Hanover, NH 03755</p>

<u>No. of</u> <u>Copies</u>	<u>Organization</u>
1	<p>Director U.S. Army Research Laboratory ATTN: AMSRL-WT-L, D. Woodbury 2800 Powder Mill Road Adelphi, MD 20783-1145</p>
3	<p>Commander U.S. Army Missile Command ATTN: AMSMI-RD, W. McCorkle AMSMI-RD-ST, P. Doyle AMSMI-RD-ST-CN, T. Vandiver Redstone Arsenal, AL 35898</p>
2	<p>U.S. Army Research Office Dir., Math & Computer Sciences Div. ATTN: Andrew Crowson J. Chandra P.O. Box 12211 Research Triangle Park, NC 27709-2211</p>
1	<p>U.S. Army Research Office Engineering Sciences Div ATTN: G. Anderson P.O. Box 12211 Research Triangle Park, NC 27709-2211</p>
2	<p>Project Manager SADARM Picatinny Arsenal, NJ 07806-5000</p>
2	<p>Project Manager Tank Main Armament Systems ATTN: SFAE-AR-TMA, COL Bregard C. Kimker Picatinny Arsenal, NJ 07806-5000</p>
3	<p>Project Manager Tank Main Armament Systems ATTN: SFAE-AR-TMA-MD, H. Yuen J. McGreen R. Kowalski Picatinny Arsenal, NJ 07806-5000</p>
2	<p>Project Manager Tank Main Armament Systems ATTN: SFAE-AR-TMA-MS, R. Joinson D. Guziewicz Picatinny Arsenal, NJ 07806-5000</p>

<u>No. of Copies</u>	<u>Organization</u>	<u>No. of Copies</u>	<u>Organization</u>
1	Project Manager Tank Main Armament Systems SFAE-AR-TMA-MP, W. Lang Picatinny Arsenal, NJ 07806-5000	1	Office of Naval Research Mech Div Code 1132SM ATTN: Yapa Rajapakse Arlington, VA 22217
2	PEO-Armaments ATTN: SFAE-AR-PM, D. Adams T. McWilliams Picatinny Arsenal, NJ 07806-5000	1	Naval Ordnance Station Advanced Systems Technology Br. ATTN: D. Holmes Code 2011 Louisville, KY 40214-5245
1	PEO-Field Artillery Systems ATTN: SFAE-FAS-PM, H. Goldman Picatinny Arsenal, NJ 07806	1	David Taylor Research Center Ship Structures and Protection Department ATTN: J. Corrado, Code 1702 Bethesda, MD 20084
4	Project Manager, AFAS ATTN: LTC D. Ellis G. delCoco J. Shields B. Machak Picatinny Arsenal, NJ 07806-5000	2	David Taylor Research Center ATTN: R. Rockwell W. Phyllaier Bethesda, MD 20054-5000
2	Commander DARPA ATTN: J. Kelly B. Wilcox 3701 North Fairfax Drive Arlington, VA 22203-1714	5	Director Lawrence Livermore National Laboratory ATTN: R. Christensen S. deTeresa W. Feng F. Magness M. Finger P.O. Box 808 Livermore, CA 94550
2	Commander Wright-Patterson Air Force Base ATTN: WL/FIV, A. Mayer Dayton, OH 45433	1	Director Los Alamos National Laboratory ATTN: D. Rabern MEE-13, Mail Stop J-576 P.O. Box 1633 Los Alamos, NM 87545
2	NASA Langley Research Center Mail Stop 266 ATTN: AMSRL-VS, W. Elber F. Barlett, Jr. Hampton, VA 23681-0001	1	Oak Ridge National Laboratory ATTN: R. M. Davis P.O. Box 2008 Oak Ridge, TN 37831-6195
2	Naval Surface Warfare Center Dahlgren Division Code G33 Dahlgren, VA 224488	1	Pacific Northwest Laboratory ATTN: M. Smith P.O. Box 999 Richland, WA 99352
1	Naval Research Laboratory Code 6383 ATTN: I. Wolock Washington, DC 20375-5000		

<u>No. of Copies</u>	<u>Organization</u>	<u>No. of Copies</u>	<u>Organization</u>
6	Director Sandia National Laboratories Applied Mechanics Department, Division-8241 ATTN: C. Robinson G. Benedetti W. Kawahara K. Perano D. Dawson P. Nielan P.O. Box 969 Livermore, CA 94550-0096	1	UCLA MANE Dept, Engrg IV ATTN: H. Thomas Hahn Los Angeles, CA 90024-1597
1	Drexel University ATTN: Albert S.D. Wang 32nd and Chestnut Streets Philadelphia, PA 19104	2	Univ of Dayton Research Inst ATTN: Ran Y. Kim Ajit K. Roy 300 College Park Avenue Dayton, OH 45469-0168
2	North Carolina State University Civil Engineering Department ATTN: W. Rasdorf L. Spainhour P.O. Box 7908 Raleigh, NC 27696-7908	1	University of Dayton ATTN: James M. Whitney 300 College Park Ave Dayton, OH 45469-0240
1	Pennsylvania State University ATTN: David W. Jensen 223-N Hammond University Park, PA 16802	2	University of Delaware Center for Composite Materials ATTN: J. Gillespe M. Santare 201 Spencer Laboratory Newark, DE 19716
1	Pennsylvania State University ATTN: Richard McNitt 227 Hammond Bldg University Park, PA 16802	1	University of Illinois at Urbana-Champaign National Center for Composite Materials Research 216 Talbot Laboratory ATTN: J. Economy 104 South Wright Street Urbana, IL 61801
1	Pennsylvania State University ATTN: Renata S. Engel 245 Hammond Building University Park, PA 16801	1	University of Kentucky ATTN: Lynn Penn 763 Anderson Hall Lexington, KY 40506-0046
1	Purdue University School of Aero & Astro ATTN: C.T. Sun W. Lafayette, IN 47907-1282	1	The University of Texas at Austin Center for Electromechanics ATTN: J. Price 10100 Burnet Road Austin, TX 78758-4497
1	Stanford University Department of Aeronautics and Aeroballisticss Durant Building ATTN: S. Tsai Stanford, CA 94305	1	University of Utah Department of Mechanical and Industrial Engineering ATTN: S. Swanson Salt Lake City, UT 84112

<u>No. of Copies</u>	<u>Organization</u>
2	Virginia Polytechnical Institute & State University Dept of ESM ATTN: Michael W. Hyer Kenneth L. Reifsnider Blacksburg, VA 24061-0219
1	AAI Corporation ATTN: J. Hebert P.O. Box 126 Hunt Valley, MD 21030-0126
1	ARMTEC Defense Products ATTN: Steve Dyer 85-901 Avenue 53 P.O. Box 848 Coachella, CA 92236
2	Advanced Composite Materials Corporation ATTN: P. Hood J. Rhodes 1525 S. Buncombe Road Greer, SC 29651-9208
3	Alliant Techsystems, Inc. ATTN: C. Candland J. Bode K. Ward 5901 Lincoln Dr. Minneapolis, MN 55346-1674
1	Alliant Techsystems, Inc Precision Armaments Systems Group 7225 Northland Drive Brooklyn Park, MN 55428
1	Amoco Performance Products, Inc. ATTN: M. Michno, Jr. 4500 McGinnis Ferry Road Alpharetta, GA 30202-3944
1	Applied Composites ATTN: W. Grisch 333 North Sixth Street St. Charles, IL 60174

<u>No. of Copies</u>	<u>Organization</u>
1	Brunswick Defense ATTN: T. Harris Suite 410 1745 Jefferson Davis Hwy. Arlington, VA 22202
1	Chamberlain Manufacturing Corporation Research and Development Division ATTN: T. Lynch P.O. Box 2335 550 Esther Street Waterloo, IA 50704
1	Chamberlain Manufacturing Corporation Research and Development Division ATTN: M. Townsend P.O. Box 2545 550 Esther Street Waterloo, IA 50704
1	Custom Analytical Engineering Systems, Inc. ATTN: A. Alexander Star Route, Box 4A Flintstone, MD 21530
1	General Dynamics Land Systems Division ATTN: D. Bartle P.O. Box 1901 Warren, MI 48090
3	Hercules, Incorporated ATTN: R. Boe F. Policelli J. Poesch P.O. Box 98 Magna, UT 84044
3	Hercules, Incorporated ATTN: G. Kuebler J. Vermeychuk B. Manderville, Jr. Hercules Plaza Wilmington, DE 19894

<u>No. of Copies</u>	<u>Organization</u>	<u>No. of Copies</u>	<u>Organization</u>
1	Hexcel ATTN: M. Shelendich 11555 Dublin Blvd. P.O. Box 2312 Dublin, CA 94568-0705	1	Olin Corporation ATTN: L. Whitmore 10101 9th St., North St. Petersburg, FL 33702
1	IAP Research, Inc. ATTN: A. Challita 2763 Culver Avenue Dayton, Ohio 45429	1	Rensselaer Polytechnic Institute ATTN: R. B. Pipes Troy, NY
2	Institute for Advanced Technology ATTN: T. Kiehne H. Fair P. Sullivan 4030-2 W. Braker Lane Austin, TX 78759	1	SPARTA, Inc. ATTN: J. Glatz 9455 Towne Centre Drive San Diego, CA 92121-1964
1	Integrated Composite Technologies ATTN: H. Perkinson, Jr. P.O. Box 397 York New Salem, PA 17371-0397	2	United Defense LP ATTN: P. Para G. Thomas 1107 Coleman Avenue, Box 367 San Jose, CA 95103
1	Interferometrics, Inc. ATTN: R. Larriva, Vice President 8150 Leesburg Pike Vienna, VA 22100		<u>Aberdeen Proving Ground</u>
3	LORAL/Vought Systems ATTN: G. Jackson K. Cook L.L. Hadden 1701 West Marshall Drive Grand Prairie, TX 75051	73	Dir, USARL ATTN: AMSRL-CI, C. Mermegan (394) AMSRL-CI-C, W. Sturek (1121) AMSRL-CI-CB, R. Kaste (394) AMSRL-CI-S, A. Mark (309) AMSRL-SL-B, P. Dietz (328) AMSRL-SL-BA, J. Walbert (1065) AMSRL-SL-BL, D. Bely (328) AMSRL-SL-I, D. Haskill (1065) AMSRL-WT-P, A. Horst (390A) AMSRL-WT-PA, T. Minor (390) C. Leveritt (390) D. Kooker (390A) AMSRL-WT-PB, E. Schmidt (120) P. Plostins (120) AMSRL-WT-PC, R. Fifer (390A)
2	Martin-Marietta Corp. ATTN: P. Dewar L. Sponar 230 East Goddard Blvd. King of Prussia, PA 19406		
2	Olin Corporation Flinchbaugh Division ATTN: E. Steiner B. Stewart P.O. Box 127 Red Lion, PA 17356		

**No. of
Codes Organization**

AMSRL-WT-PD,
B. Burns (390)
W. Drysdale (390)
K. Bannister (390)
T. Bogetti (390)
J. Bender (390)
R. Murray (390)
R. Kirkendall (390)
T. Erline (390)
D. Hopkins (390)
S. Wilkerson (390)
C. McCall (390)
D. Henry (390)
R. Kaste (390)
L. Burton (390)
J. Tzeng (390)
R. Lieb (390)
G. Gazonas (390)(10 cp)
M. Leadore (390)
C. Hoppel (390)
AMSRL-WT-PD(ALC),
A. Abrahamian
K. Barnes
M. Berman
H. Davison
A. Frydman
T. Li
W. McIntosh
E. Szymanski
AMSRL-WT-T, W. Morrison (309)
AMSRL-WT-TA,
W. Gillich (390)
W. Bruchey (390)
AMSRL-WT-TC,
K. Kimsey (309)
R. Coates (309)
W. de Rosset (309)
AMSRL-WT-TD,
D. Dietrich (309)
G. Randers-Pehrson (309)
J. Huffington (309)
A. Das Gupta (309)
J. Santiago (309)
AMSRL-WT-W, C. Murphy (120)
AMSRL-WT-WA,
H. Rogers (394)
B. Moore (394)
A. Baran (394)

**No. of
Codes Organization**

AMSRL-WT-WB,
F. Brandon (120)
W. D'Amico (120)
AMSRL-WT-WC,
J. Rocchio (120)
AMSRL-WT-WD,
A. Zielinski (120)
J. Powell (120)
AMSRL-WT-WE,
J. Temperley (120)
J. Thomas (394)

USER EVALUATION SHEET/CHANGE OF ADDRESS

This Laboratory undertakes a continuing effort to improve the quality of the reports it publishes. Your comments/answers to the items/questions below will aid us in our efforts.

1. ARL Report Number ARL-TR-469 Date of Report June 94

2. Date Report Received _____

3. Does this report satisfy a need? (Comment on purpose, related project, or other area of interest for which the report will be used.) _____

4. Specifically, how is the report being used? (Information source, design data, procedure, source of ideas, etc.) _____

5. Has the information in this report led to any quantitative savings as far as man-hours or dollars saved, operating costs avoided, or efficiencies achieved, etc? If so, please elaborate. _____

6. General Comments. What do you think should be changed to improve future reports? (Indicate changes to organization, technical content, format, etc.) _____

**CURRENT
ADDRESS**

Organization

Name

Street or P.O. Box No.

City, State, Zip Code

7. If indicating a Change of Address or Address Correction, please provide the Current or Correct address above and the Old or Incorrect address below.

**OLD
ADDRESS**

Organization

Name

Street or P.O. Box No.

City, State, Zip Code

(Remove this sheet, fold as indicated, tape closed, and mail.)
(DO NOT STAPLE)

DEPARTMENT OF THE ARMY



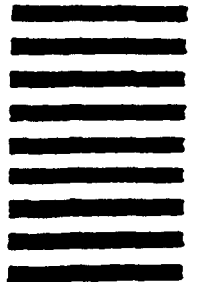
OFFICIAL BUSINESS

BUSINESS REPLY MAIL

FIRST CLASS PERMIT No 0001, APG, MD

Postage will be paid by addressee.

**NO POSTAGE
NECESSARY
IF MAILED
IN THE
UNITED STATES**



**Director
U.S. Army Research Laboratory
ATTN: AMSRL-OP-CI-B (Tech Lib)
Aberdeen Proving Ground, MD 21005-5066**